Geological Survey of Canada

CURRENT RESEARCH

2004-C4

Pore-size distribution for graphitic shale samples from the Astarte River formation, Piling Group, Baffin Island, Nunavut

S. Connell-Madore, J. Li, and K. Dexter

2004

Natural Resources
Canada

Ressources naturelles
Canada

Canada

Authors' addresses

S. Connell-Madore (sconnell@nrcan.gc.ca)
K. Dexter
Geological Survey of Canada
601 Booth Street
Ottawa, Ontario K1A 0E8

J. Li (jili@nrcan.gc.ca)
Materials Technology Laboratory - CANMET
568 Booth Street
Ottawa, Ontario K1A 0G1

Pore-size distribution for graphitic shale samples from the Astarte River formation, Piling Group, Baffin Island, Nunavut

S. Connell-Madore, J. Li, and K. Dexter

Abstract: Pore-size distribution analysis was performed on four graphitic shale samples from the Astarte River formation, Baffin Island, Nunavut. This included measurement and interpretation of pore-size distribution data obtained by mercury injection porosimetry. The purpose was to document the results of the pore-size analysis and to provide pore-structure information on the graphitic shale. These would eventually be used for electrical mechanism analysis and geophysical survey interpretation.

Effective porosity values determined by mercury porosimetry (ϕ_{Hg1} and ϕ_{Hg2}) were in the ranges of 3.47–14.2%. The storage and connecting porosity values (ϕ_s and ϕ_c) were in the ranges of 2.72–12.8% and 1.03–2.29%, respectively. The sulphide-rich samples have the lowest porosity values (3.5–4.2%). The samples with higher porosities (sample numbers BAF-1 and BAF-2) have pore-size distribution patterns that resemble those of typical mudstone. The samples with lower porosity values (BAF-3 and BAF-AB) have more similarities to crystalline rocks.

Résumé : On a analysé la distribution de la taille des pores dans quatre échantillons de shale graphitique de la formation d'Astarte River, dans l'île de Baffin (Nunavut). L'analyse a englobé la mesure et l'interprétation des données sur la distribution de la taille des pores obtenues par porosimétrie par injection de mercure. L'étude avait comme objet de documenter les résultats de l'analyse de la taille des pores et de fournir de l'information sur la structure des vides dans le schiste à muscovite, quartz et graphite. Ces données serviront ultérieurement pour l'analyse des mécanismes électriques et l'interprétation de levés géophysiques.

Les valeurs de la porosité efficace, déterminées par porosimétrie par injection de mercure (ϕ_{Hg1} et ϕ_{Hg2}), étaient de l'ordre de 3,47 à 14,2 %. Les valeurs de la porosité close (ϕ_s) étaient de l'ordre de 2,72 à 12,8 % et celles de la porosité ouverte (ϕ_c), de l'ordre de 1,03 à 2,29 %. Les échantillons riches en sulfures présentaient les valeurs de porosité les plus faibles (de 3,5 à 4,2 %). Les échantillons dont les valeurs de porosité étaient plus élevées (échantillons BAF-1 et BAF-2) présentaient des configurations de distribution de la taille des pores semblables à celles d'un mudstone typique. Les échantillons présentant des valeurs de porosité moins élevées (BAF-3 et BAF-AB) sont davantage similaires aux roches cristallines.
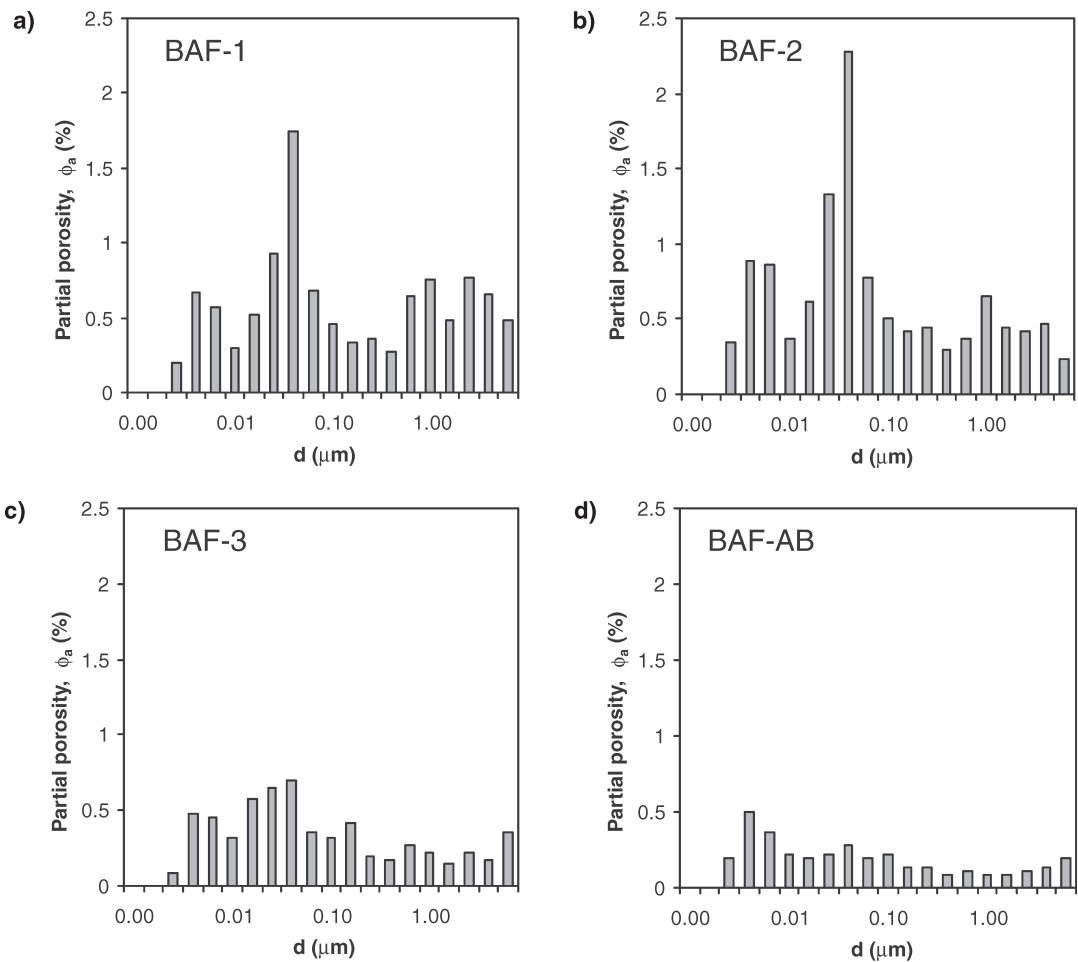
INTRODUCTION

Pore-size distribution analysis was performed on four graphitic shale samples from the Astarte River formation, Baffin Island, Nunavut. These four samples were provided by Alan Jones (GSC). This study includes analysis and interpretation of pore-size distribution data obtained by mercury injection porosimetry measurements, which is essential for the electrical mechanism analysis of these shale samples. The purpose of this paper is to document, within the framework of the Central Baffin Project, results of pore-size analysis and to provide pore-structure information on the graphite-rich shale samples.

Table 1. Sample descriptions.

Group	Sample number	Description	Sulphides
I	BAF-1	Strong foliation, fissile, porous lenses	Trace
	BAF-2		Trace
II	BAF-3	Strong foliation, fissile, porous layers	Trace
	BAF-AB	Weak to moderate foliation, fine-grained disseminated euhedral sulphides with poor connectivity	3–5%

Figure 1. Pore-size distribution plots for sample a) BAF-1, b) BAF-2, c) BAF-3, and d) pyritic BAF-AB.

This information would eventually be used to assist in interpreting ground electromagnetic surveys which have been conducted in the area.

METHOD OF INVESTIGATION

Specimens from each of the four samples (as listed in Table 1, Fig. 1) were prepared for mercury injection porosimetry testing by AGAT Laboratories (Calgary, Alberta). At AGAT Laboratories, each specimen was oven dried at 80°C, then individually placed in a penetrometer assembly under vacuum. The penetrometer was then filled with mercury at a hydrostatic head of approximately 10 kPa. The volume of the mercury injected is recorded after stabilization at each pressure step up to 414 MPa (60 000 psi) at which time the mercury is assumed to have accessed connecting pores as small as 2.5–3.0 nm. Further details of the procedures are described elsewhere (Katsube et al., 1997, 1998).

Separate specimens from each sample were also prepared for image analysis study using a scanning electron microscope (SEM), and the results reported elsewhere (Connell-Madore et al., 2004). Secondary and backscatter images are used for a detailed analysis on the electrical mechanisms of these shale samples in that study. Secondary SEM images of samples BAF-3 and BAF-AB (Fig. 2, 3) from that study are included in this paper, because they contain unusually large pores.
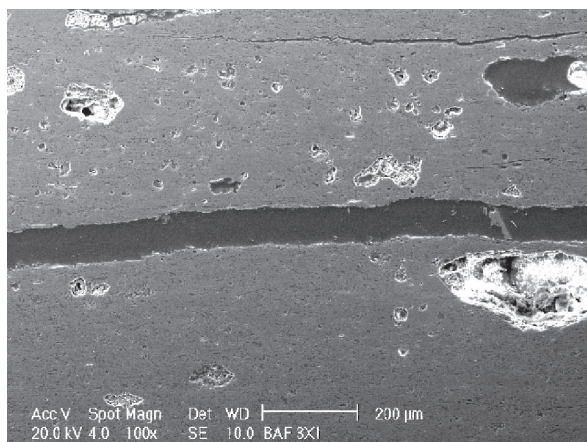
ANALYTICAL RESULTS

The results of the mercury injection porosimetry tests are listed in Table 2. The results are also plotted in a standard format (Fig. 1) where one decade of pore sizes are divided into five cells of equal physical spacing (Katsube and Issler, 1993). The partial porosity, ϕ_a (Fig. 1, 4; Table 2), is the porosity of each cell or the porosity contributed by each pore-size range. The pore-size parameter, d_a, is the geometric mean for each cell or pore-size range (in nanometres). The data for the bulk parameters derived from the pore-size distributions are listed in the lower section of the table. They represent mercury porosities (ϕ_{Hg1}, ϕ_{Hg2}), bulk density (δ_{BD}), skeletal density (δ_{SD}), pore surface area (A), residual or storage porosity (ϕ_s), residual porosity ratio (ϕ_{rr}), connecting porosity (ϕ_c), and mode of pore-size distribution (d_m) of the dry sample. The definition of these parameters can be found elsewhere (Katsube et al., 1997, 1998) and also in Table 2 for ϕ_{Hg1} and ϕ_{Hg2}. Normally, for shale or any other fine-grained rocks, ϕ_{Hg1} is used in the determination of storage and connecting porosity. This is because ϕ_{Hg1} excludes pore sizes that exceed 10 µm, and eliminates measurement error in determining pore spaces between the specimen and container (Katsube and Issler, 1993); however, since large pore spaces are visible in these hand samples (e.g. Fig. 2, 3), ϕ_{Hg2} is used in the connecting and storage porosity calculations. It is judged that the measurement errors are not significant in this case.
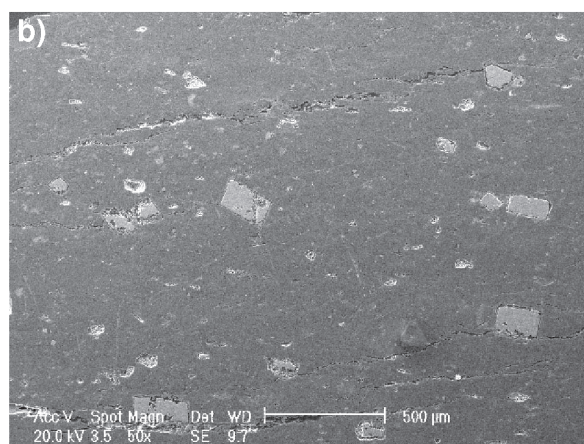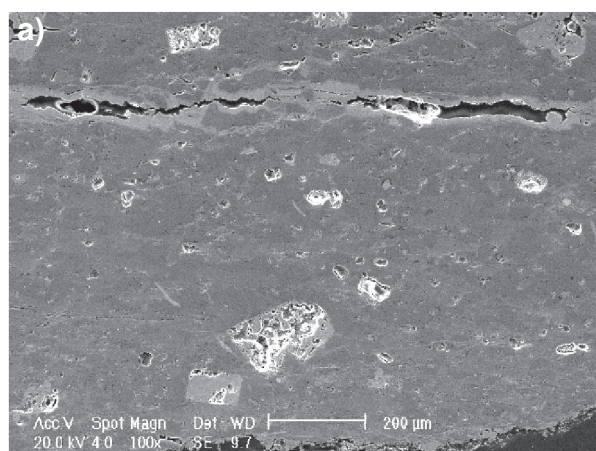
Table 2. Pore-size distribution data for different pore-size ranges, d_a, obtained by mercury porosimetry for Astarte River formation, black shale samples.

d_a (nm)	BAF-1	BAF-2	BAF-3	BAF-AB
	ϕ_a (%)			
3.2	0.2	0.34	0.09	0.19
5.0	0.67	0.89	0.48	0.50
7.9	0.57	0.86	0.45	0.36
12.6	0.3	0.37	0.32	0.22
20.0	0.52	0.61	0.57	0.19
31.6	0.93	1.33	0.65	0.22
50.1	1.75	2.28	0.70	0.28
79.4	0.68	0.77	0.35	0.19
126	0.46	0.51	0.32	0.22
200	0.34	0.42	0.42	0.14
316	0.36	0.44	0.20	0.14
501	0.27	0.30	0.17	0.08
794	0.64	0.37	0.27	0.11
1259	0.75	0.65	0.22	0.08
1995	0.48	0.44	0.15	0.08
3162	0.77	0.42	0.22	0.11
5012	0.66	0.47	0.17	0.14
7943	0.48	0.23	0.35	0.19
ϕ_{Hg1}	10.85	11.72	6.12	3.47
ϕ_{Hg2}	14.22	14.10	7.68	4.19
d_{hg}	616.1	248.4	309.6	194.2
d_{BD}	2.28	2.33	2.49	2.78
d_{SD}	2.66	2.72	2.69	2.99
A	6.29	8.615	4.095	3.23
ϕ_s	12.87	11.81	6.66	2.72
ϕ_{rr}	0.91	0.84	0.87	0.65
ϕ_c	1.35	2.29	1.03	1.47
d_m	50.1	50.1	50.1	5.0

d_a = Geometric mean pore sizes for the different pore-size ranges (nm).

d_{hg} = Geometric mean of the entire pore-size distribution (nm).

ϕ_a = Partial porosity (%).

ϕ_{Hg1} = Total porosity measured by mercury porosimetry for pore sizes up to 10 µm (%).

ϕ_{Hg2} = Total porosity measured by mercury porosimetry for pore sizes up to 250 µm (%).

δ_{BD} = Bulk density (g/mL).

δ_{SD} = Skeletal density (g/mL).

A = Surface area (m^2/g).

ϕ_s = Storage porosity (%).

ϕ_{rr} = Residual or isolated porosity (%).

ϕ_c = Connecting porosity (%).

d_m = Pore size of the major pore-size mode, d (nm).

Figure 2. Scanning electron microscope image in secondary light illustrating some larger pores in sample BAF-3 that would appear to have good connectivity. The dark line though the middle is a fracture filled with epoxy.

Figure 3. Scanning electron microscope images in secondary light of a polished surface for sample for BAF-AB illustrating a) an alteration halo along a bedding-plane fracture and a), b) degradation of pyrite grains.
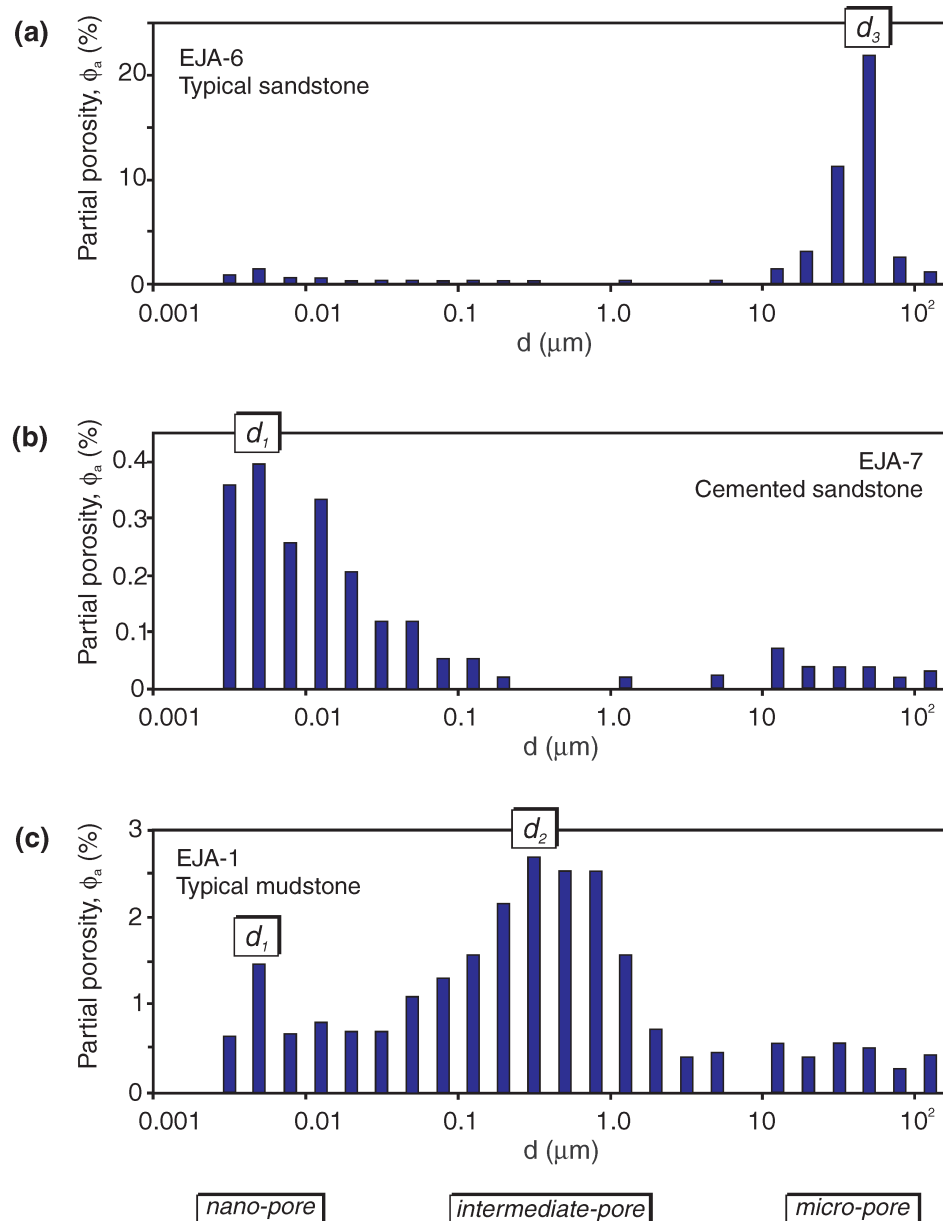
DISCUSSION AND CONCLUSIONS

Pore-size distribution patterns for some typical sedimentary rock types are displayed in Figure 4 (Katsube et al., 1999). There are three pore-size ranges ('nano-pore', 'intermediate-pore', and 'micro-pores') with the common modes for mudstone being in the nano-pore and intermediate-pore size range (Fig. 4c). The porosity values and pore-size distribution pattern for samples BAF-1 and BAF-2 (Fig. 1a, b) are similar to that seen in Figure 4c of a typical mudstone. The porosity values for BAF-3 and BAF-AB are much lower and resemble the distribution patterns of crystalline rocks more than sedimentary rocks (Connell, 2001).

The mercury porosity values (ϕ_{Hg1} and ϕ_{Hg2}) determined by mercury porosimetry are in the ranges from 3.47% to 14.22%. The ϕ_s, ϕ_{rr}, and ϕ_c are in the ranges of 2.72% to 12.87%, 0.65% to 0.91%, and 1.03% to 2.29%, respectively (Table 2). There are two prominent modes visible in the pore-size distribution plots: nano-pore and intermediate-pore size ranges (5 nm and 50 nm). This distribution pattern is typical of mudstone (Fig. 4c) with similar modes of d_1 and d_2. The pore-size distribution patterns can be divided into two groups.

Group I (Fig. 1a, b) represented by BAF-1 and BAF-2 and group II (Fig. 1c, d) represented by BAF-3 and BAF-AB. Group I samples have nearly identical bimodal pore-size distributions with pore-size modes at 0.006 µm and 0.04 µm. The storage porosities are considerably higher for these samples at 12.87% and 11.81%, compared to 6.66% and 2.72% of group II samples. The group II samples have similar pore-size distributions with similar modes, but they are not clearly defined. The maximum partial porosity (ϕ_a) reached for BAF-AB and BAF-3 is only 0.7%, whereas the maximum ϕ_a for the group I samples is 2.28%.

Sample BAF-1 (14.2%) showed the highest porosity of all four. Sample BAF-AB (3.47%) showed the lowest porosity which is likely a result of the sulphide minerals infilling some of the pore spaces, and may have undergone some type of alteration.

Scanning electron microscope images in secondary light (showing relief) for samples BAF-3 (Fig. 2) and BAF-AB (Fig. 3a, b) give an indication of the type of porosity present. The primary pore type appears to be bedding-plane fractures (grain boundary pores parallel to bedding), which facilitate

Figure 4. *Typical pore-size distribution plots of a) sandstone, b) tight sandstone, and c) mudstone samples. The d₁, d₂, and d₃ are the modes for each of the three pore-size distribution bodies. This figure has been* modified from *Katsube et al. (1999).*

the movement of water that would create dissolution pores. Figure 2 shows a large fracture that has been filled with epoxy during the polishing process. There are other pores that were not infilled that do appear to have some interconnectivity. Degradation of pyrite grains is evident in Figure 3a and 3b which may have resulted from the preferential leeching of impurities in the grains. An alteration halo is evident along the bedding-plane fracture in the top section of Figure 3a. Results and further details of the SEM analysis and on the electrical mechanisms of these shale samples can be found elsewhere (Connell-Madore et al., 2004).

REFERENCES

Connell, S.
2001: Pore-size distribution characteristics of Yellowknife mining district rocks, Northwest Territories; Geological Survey of Canada, Current Research 2001-E1, 7 p.

Connell-Madore, S., Hunt, P., and Li, J.
2004: Electrical conductivity mechanism of graphitic shale from the Astarte River formation, Piling Group, Baffin Island, Nunavut; *in* Geological Survey of Canada, Current Research 2004-C5.

Katsube, T.J. and Issler, D.R.
1993: Pore-size distribution of shales from the Beaufort-Mackenzie Basin, northern Canada; *in* Current Research, Part E; Geological Survey of Canada, Paper 93-1E, p. 123–132.

Katsube, T.J., Cox, W.C., and Issler, D.R.
1998: Porosity characteristics of shale formations from the Western Canada Sedimentary Basin; *in* Current Research 1998-E; Geological Survey of Canada, p. 63–74.

Katsube, T.J., Dallimore, S.R., Uchida, T., Jenner, K.A., Collett, T.S., and Connell, S.
1999: Petrophysical environment of sediments hosting gas-hydrate, JAPEX/JNOC/GSC Mallik 2L-38 gas hydrate research well; *in* Scientific Results from JAPEX/JNOC/GSC Mallik 2L-38 Gas Hydrate Research Well, Mackenzie Delta, Northwest Territories, Canada, (ed.) S.R. Dallimore, T. Uchida, and T.S. Collett; Geological Survey of Canada, Bulletin 544, p. 109–124.

Katsube, T.J., Dorsch, J., and Connell, S.
1997: Pore surface area characteristics of the Nolichucky Shale within the Oak Ridge Reservation (Tennessee, USA): implication for fluid expulsion efficiency; *in* Current Research 1997-E; Geological Survey of Canada, p. 117–124.

Geological Survey of Canada Project Y14